# Nanocrystalline hydroxyapatite-based scaffold adsorbs and gives sustained release of osteoinductive growth factor and facilitates bone regeneration in mice ectopic model

Zhou, M.; Geng, Y.M.; Li, S.Y.; Yang, X.B.; Che, Y.J.; Pathak, J.L.; Wu, G.

**DOI**
10.1155/2019/1202159

**Publication date**
2019

**Document Version**
Final published version

**Published in**
Journal of Nanomaterials

Hindawi
Journal of Nanomaterials
Volume 2019, Article ID 1202159, 10 pages
https://doi.org/10.1155/2019/1202159

*Research Article*

# Nanocrystalline Hydroxyapatite-Based Scaffold Adsorbs and Gives Sustained Release of Osteoinductive Growth Factor and Facilitates Bone Regeneration in Mice Ectopic Model

**Miao Zhou,[1] Yuan-ming Geng,[2] Shu-yi Li,[1] Xiao-bin Yang,[1] Yue-juan Che,[3] Janak Lal Pathak,[1] and Gang Wu[4]**

[1]*Key Laboratory of Oral Medicine, Guangzhou Institute of Oral Disease, Affiliated Stomatology Hospital of Guangzhou Medical University, Guangzhou 510140, China*
[2]*Department of Stomatology, Zhujiang Hospital, Southern Medical University, Guangzhou 510282, China*
[3]*Department of Anesthesia, Sun Yat-Sen Memorial Hospital, Sun Yat-Sen University, Guangzhou 510120, China*
[4]*Department of Oral Implantology and Prosthetic Dentistry, Academic Centre for Dentistry Amsterdam (ACTA), Universiteit van Amsterdam and Vrije Universiteit Amsterdam, Amsterdam 1081LA, Netherlands*

Correspondence should be addressed to Yue-juan Che; moon3173@163.com and Janak Lal Pathak; janakpathak@163.com

Received 22 August 2018; Revised 25 October 2018; Accepted 6 November 2018; Published 22 January 2019

Academic Editor: Rajesh R. Naik



Nanocrystalline hydroxyapatite (NHA) is a biocompatible, biodegradable, and osteoconductive bone graft material; however, it lacks osteoinductivity. The present study is aimed at investigating the feasibility of nanocrystalline hydroxyapatite (NHA) as an osteoinductive growth factor carrier. Bone morphogenic protein 2 (BMP2), an osteoinductive growth factor, was incorporated into NHA (BMP2-NHA) using a simple adsorption method. The growth factor loading and release kinetics were profiled using fluorescein-isothiocyanate-labeled bovine serum albumin (FITC-BSA) as a mimic of the osteoinductive growth factor BMP2. The effect of BMP2-NHA on the osteogenic differentiation of C2C12 cells and ectopic bone formation in mice were tested. Confocal laser-scanning microscopy showed that FITC-BSA was diffused throughout the porous structure of NHA. FITC-BSA was efficiently loaded in NHA and sustained release was observed up to 35 days in vitro. BMP2-NHA enhanced the expression of osteogenic markers *Runx2*, *Osterix*, *Alp*, and *Col1α1* and ALP activity in C2C12 cells compared to NHA. Similarly, $\mu$-CT and histological examinations showed that BMP2-NHA robustly induced ectopic bone formation in mice. This study suggests that NHA could be used as an effective carrier of osteoinductive growth factors, which ensures osteoinductivity of NHA via sustained release of the growth factor.

## 1. Introduction

Large-volume bone defects resulting from tumors, trauma, infection, and congenital deformity exceed the self-healing capacity of natural bone tissue. The repair of such defects remains a challenge in the field of orthopedics, dental implantology, and maxillofacial surgery. Autograft is still regarded as the gold-standard treatment option for large-volume bone defects [1]. The osteogenic potential of autografts is derived from their osteoconductive scaffold, osteoinductive growth factors (such as bone morphogenetic proteins, BMPs), and osteogenic precursor cells. However, the application of autografts is still limited by availability and donor site morbidity [2]. The conventional alternatives such as allografts and xenografts (e.g., deproteinized bovine bone) are also associated with concerns of immunologic reaction and potential disease transmission [3, 4]. In comparison, synthetic calcium phosphate- (CaP-) based materials show unlimited availability, no risk of potential disease transmission, and great modification potential to be conferred with advanced properties [5]. Synthetic materials such as tricalcium phosphate (TCP) and biphasic calcium phosphate (BCP) have already been widely used in clinical settings [6–11]. These synthetic materials could be further functionalized

with a paramount property—osteoinductivity—by a very simple way that is called superficial adsorption of BMP2 [12]. Such functionalized CaP-based materials have been shown to enhance bone regeneration in animal studies [13, 14]. However, this functionalization method is associated with a low osteoinductive efficiency since the superficially adsorbed BMP2 is rapidly released and exhausted in the physiological milieu before taking an osteoinductive effect [15, 16]. Moreover, the physicochemical properties of TCP or BCP could not provide a slow release system to BMPs [17, 18]. Therefore, BMPs have to be administrated in supraphysiologic dosages to induce satisfactory bone formation, which in turn lead to concerns of bone overgrowth, cost-effectiveness considerations, and significant complications [19]. To optimize the osteoinductive efficiency of BMPs, the scaffold materials should bear a good capacity to retain their activities and to enable a sustained local release [20].

Among the synthetic materials that are available in clinical settings, nanocrystalline hydroxyapatite- (NHA-) based scaffolds, such as NanoBone® (Artoss, Rostock, Germany), appear to be promising materials for the adsorption and sustained release of osteoinductive growth factors. This NHA-based scaffold consists of 76% nanocrystalline hydroxyapatite that is embedded in nanostructured silica using a sol-gel method. This material bears a porosity of 60–80%, macropore size of some 100 mm, nanopore size of 10–20 nm, and large surface area exceeding 84 $m^2$/g [21, 22]. Silica not only gives higher porosity and surface area but also enhances the osteoinductive properties of NHA. Previous studies had reported that a silica-based scaffold shows higher biocompatibility and osteogenic properties [23, 24]. Moreover, a silica-coated titanium implant enhances osteogenic differentiation of precursor cells [25]. NHA gains quite satisfactory outcomes in clinical situations including socket preservation and sinus augmentation [26–28]. The characteristics of NHA favored for bone regeneration, such as biocompatibility, biodegradability, osteoconductivity, and angiogenic response, are well documented [29–31]. However, NHA lacks osteoinductivity and it remains unclear whether the NHA-based scaffold with such a significantly enlarged surface area is able to efficiently adsorb osteoinductive growth factors and give sustained local release.

In this study, we tested the loading efficiency and release profile of proteinous agents adsorbed in the clinically used NHA-based scaffold. We evaluated the osteoinductive efficacy of BMP2-adsorbed NHA both in in vitro and in vivo subcutaneous bone-induction models in mice.

## 2. Materials and Methods

*2.1. Drug Loading.* FITC-BSA (Sigma-Aldrich, St. Louis, MO, USA) was used as a model protein to monitor the loading efficiency and release kinetics of osteoinductive growth factors. FITC-BSA was dissolved in PBS at 0.05 mg/ml (low concentration, L-BSA-NHA), 0.25 mg/ml (medium concentration, M-BSA-NHA), and 1.25 mg/ml (high concentration, H-BSA-NHA), respectively. NHA blocks (NanoBone®) were trimmed to $4 \times 4 \times 4$ mm blocks. Each block was immersed in 0.4 ml of FITC-BSA solution separately. The blocks were vortexed once per minute at 4°C for 24 h and then dried at 4°C for 24 h. The supernatants were collected for analysis of loading efficiency. The fluorescence density was measured with a microplate reader (Varioskan Flash, Thermo Fisher Scientific, Waltham, MA, USA) at an excitation wavelength of 485 nm and emission wavelength of 519 nm. FITC-BSA concentration in the supernatant was calculated using the linear relationship with fluorescence density. The loading efficiency was calculated using the following formula:

$$\text{Loading efficiency} = 1 - \frac{C_s \times V_s}{C_0 \times V_0}, \quad (1)$$

where $C_s$ is the FITC-BSA concentration in the supernatant, $V_s$ is the volume of supernatants, $C_0$ is the original concentration of FITC-BSA, and $V_0 = 0.4$ ml.

*2.2. Distribution of FITC-BSA within NHA Blocks.* The NHA blocks loaded with 1.25 mg/ml FITC-BSA solution were dehydrated and then embedded in methylmethacrylate. Sections of 60 $\mu$m were prepared using a cutting and grinding system (Exakt, Norderstedt, Germany). The sections were inspected using a confocal laser-scanning microscope (TCS SP8, Leica Microsystems, Wetzlar, Germany).

*2.3. In Vitro Release of FITC-BSA.* Each NHA block was immersed in 4 ml phosphate buffer saline (PBS). A supernatant of 0.5 ml was collected for analysis at 3 h, 6 h, 12 h, 1 d, 2 d, 3 d, 6 d, 9 d, 16 d, 23 d, 30 d, and 37 d. The same volume of PBS was added back after each collection. The concentration of FITC-BSA was determined using the linear relationship with fluorescence density.

*2.4. In Vitro Cellular Experiments*

*2.4.1. BMP2 Incorporation.* Recombinant human BMP2 (produced in *Escherichia coli*) from the Genetic Institute of Huadong Medicine (Shanghai, China) with a purity of above 98% was used as an osteoinductive growth factor model drug. NHA blocks of $4 \times 4 \times 4$ mm were immersed in 0.4 ml of BMP2 suspended in PBS solution at final concentrations of 0.05 mg/ml (low concentration, L-BMP2-NHA group), 0.25 mg/ml (medium concentration, M-BMP2-NHA group), and 1.25 mg/ml (high concentration, H-BMP2-NHA group). Control blocks were immersed in the same volume of PBS. The blocks were vortexed once per minute at 4°C for 24 h and then dried at 4°C for 24 h. Control, L-BMP2-NHA, M-BMP2-NHA, and H-BMP2-NHA blocks were tested for in vitro and in vivo osteoinductive efficacy.

*2.4.2. Cell Seeding and Culture.* NHA blocks were placed into 6-well plates (one block per well). C2C12 mouse myoblast cells (Cell Bank of the Chinese Academy of Sciences, Shanghai, China) were seeded in the blocks ($3 \times 10^4$ cells/block in 4 ml culture medium). The cells were cocultured with the samples in $\alpha$-minimal essential medium ($\alpha$-MEM, Gibco, Grand Island, NY, USA) containing 10% fetal bovine serum (Gibco) at 37°C in a humidified atmosphere with 5% $CO_2$.

*2.4.3. Cellular Viability Assay.* Cell viability was measured using a CCK-8 (Dojindo Molecular Technologies Inc., Kumamoto, Japan) according to the manufacturer's instructions at day 7. The absorbance was measured at 450 nm using a microplate reader (Thermo Fisher Scientific).

*2.4.4. Quantitative Real-Time PCR.* Total RNA was isolated using the TRIzol Reagent (Invitrogen, Carlsbad, CA, USA) at day 7 of culture. The concentration and purity of total RNA were measured using a spectrophotometer (NanoDrop 2000, Thermo Fisher Scientific). First-strand cDNA synthesis was conducted using a HiScript® II 1st Strand cDNA Synthesis Kit (Vazyme Biotech Co. Ltd., Nanjing, China). For mRNA quantitation, an ABI 7500HT Fast Real-Time PCR System (Applied Biosystems, Foster City, CA, USA) was used with an AceQ qPCR SYBR Green Master Mix (Vazyme Biotech Co. Ltd.). Expression of *Col1α1*, *Runx2*, *Alp*, and *Osterix* mRNA in C2C12 cells was quantitated. *β*-Actin was used as a housekeeping gene. Primers used are listed in Table 1.

*2.4.5. ALP Activity Assay.* ALP activity was determined using an Alkaline Phosphatase Assay Kit (Beyotime, Shanghai, China) according to the manufacturers' instructions at day 7. The cells were harvested and lysed in 0.5% Triton X-100. Protein concentrations were measured with a BCA Protein Assay Kit (Thermo Scientific Pierce, Rockford, IL, USA). The ALP activity was normalized with total protein.

*2.5. Animal Experiments*

*2.5.1. Subcutaneous Implantation of BMP2 Incorporated NHA.* The animal study was approved by the Ethical Committee of Guangzhou Medical University, Guangzhou, China. All animal experiments were carried out according to the ethics laws and regulations of China. The test was carried out on 32 adult Kunming male mice (30–40 g body weight). Mice (8/group) were randomly divided into 4 groups: control (only NHA), L-BMP2-NHA, M-BMP2-NHA, and H-BMP2-NHA. Implants were implanted subcutaneously bilaterally in the dorsum of mice (two implants per mouse). The samples were harvested 4 weeks after the implantation.

*2.5.2. Microcomputed Tomography (μ-CT).* Bone formation was analyzed by using *μ*-CT (SkyScan high-resolution *μ*-CT imaging system, Bruker, Kontich, Belgium). The samples were scanned at 8 *μ*m resolution, 59 kV, and 100 *μ*A, with a 0.5 mm aluminum filter. Volumetric reconstruction and analysis were conducted using NRecon, CTan, and CTvox (Bruker). A threshold of 50–120 was chosen to segment out bone. The measured structural parameters were bone volume (BV), trabecular thickness (Tb.Th), trabecular separation (Tb.Sp), and trabecular number (Tb.N).

*2.5.3. Histology.* The samples were fixed in 4% paraformaldehyde. After washing with PBS, specimens were demineralized in 14% ethylenediamine tetra-acetic acid (pH = 7.2). Demineralized specimens were washed in PBS and dehydrated in a graded ethanol series. Samples were embedded in paraffin, cut into 5 *μ*m sections, and stained with Masson's trichrome. Three representative slides from each sample were photographed and analyzed for the ratio of BV/TV (bone volume/tissue volume) using Image Pro Plus 6.0 version (Media Cybernetics, Silver Spring, MD, USA).

Table 1: Primer sequences used for qPCR.

| Gene | Sequence (5′-3′) | Product length |
|---|---|---|
| *Runx2* | Forward: GACTGTGGTTACCGTCATGGC<br>Reverse: ACTTGGTTTTTCATAACAGCGGA | 84 |
| *Osterix* | Forward: AGCTCACTATGGCTCCAGTC<br>Reverse: AGGAGTCCATTGGTGCTTGA | 189 |
| *Alp* | Forward: TGGGGGCATAGACTTCAATCA<br>Reverse: CTCCGTACCAAAGCCATCAATAG | 121 |
| *Col1α1* | Forward: TTCTCCTGGCAAAGACGGAC<br>Reverse: CTCAAGGTCACGGTCACGAA | 247 |
| *β-Actin* | Forward: GGCTGTATTCCCCTCCATCG<br>Reverse: CCAGTTGGTAACAATGCCATGT | 154 |

*2.5.4. Statistical Analysis.* Statistical analysis was performed using IBM SPSS 22.0 version (IBM Corp., Armonk, NY, USA). All data were presented as mean ± SD. Statistical differences among the groups were assessed by one-way ANOVA. Post multiple comparisons were performed using the Newman-Keuls test. The significant differences between test groups and control were labeled with asterisks. The significance level was set at $p < 0.05$.

## 3. Results

*3.1. Protein Loading and Release Profiles.* After a 24 h superficial adsorption, FITC-BSA was adsorbed into NHA blocks. FITC-BSA infiltrated through the porous structure of NHA and was homogeneously distributed within the NHA blocks (Figure 1(a)). The loading efficiency of FITC-BSA was 82.35 ± 4.09%, 96.27 ± 0.36%, and 98.59 ± 0.19% in the L-BSA-NHA, M-BSA-NHA, and H-BSA-NHA groups, respectively. The release kinetics was characterized with the amount of BSA released (Figure 1(b)). The adsorbed BSA showed a sustained release from NHA blocks in all 3 groups up to 35 days.

*3.2. NHA-BMP2-Induced Osteogenic Differentiation In Vitro.* Different concentrations of BMP2-adsorbed NHA did not affect C1C12 proliferation at day 7 (Figure 2(a)). H-BMP2-NHA robustly enhanced (11.3-fold) ALP activity compared to control (Figure 2(b)). L-BMP2-NHA and M-BMP2-NHA did not affect ALP activity compared to control. Similar effects of treatments were observed in osteogenic gene expression in C2C12 cells (Figures 2(c)–2(f)). H-BMP2-NHA enhanced *Alp*, *Runx2*, *Col1α1*, and *Osterix* gene expression by 2.2-, 2.2-, 2.7-, and 12.33-fold, respectively, compared to the control group (Figures 2(c)–2(f)).

*3.3. BMP2-NHA-Enhanced Bone Formation in Mice Ectopic Model.* The 3D reconstruction images of the micro-CT scan indicated that the volume of newly formed bone significantly increased with the increase of BMP doses (Figures 3(a)–

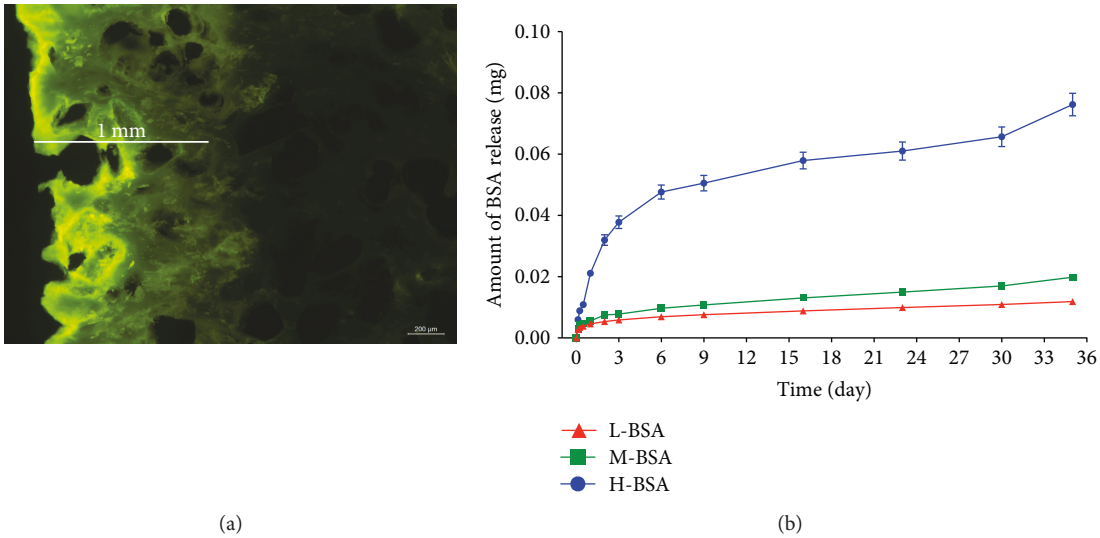


Figure 1: (a) Representative CLSM image of FITC-BSA-adsorbed NHA (scale bar: 200 $\mu$m). (b) FITC-BSA release profile. Data are presented as the mean ± SD, $n = 6$.

3(d)). Considering the whole implant, the total volume of bone (including block and newly formed bone) was significantly higher in the H-BMP2-NHA group (1.86-, 1.50-, and 1.27-fold) compared to those in the control, L-BMP2-NHA, and M-BMP2-NHA groups. Total bone volume in the M-BMP2-NHA group was 1.46-fold higher compared to those in the control group (Figure 3(e)). Tb.N in the L-BMP2-NHA, M-BMP2-NHA, and H-BMP2-NHA groups were 1.48-, 1.63-, and 1.90-fold higher compared to those in the control group (Figure 3(f)). L-BMP2-NHA, M-BMP2-NHA, and H-BMP2-NHA did not affect Tb.Th (Figure 3(g)). The M-BMP2-NHA and H-BMP2-NHA groups showed reduced Tb.Sp compared to the control and L-BMP2-NHA groups (Figure 3(h)).

The histological analysis showed that the NHA blocks alone did not yield any new bone formation in the subcutaneous sites (Figure 4(a)). In the presence of BMP2, the newly formed bone (stained in deep blue) was found surrounding the NHA blocks (stained in light blue) (Figures 4(b)–4(e)). The volume densities of newly formed bone increased with the dosage of BMP2. The bone volume densities in the M-BMP2-NHA and H-BMP2-NHA groups were 2.0- and 2.3-fold higher compared to those in the L-BMP2-NHA group (Figure 4(f)).

## 4. Discussion

Superficial adsorption is the most simple and commonly used loading method to apply BMP2 in clinical settings [32]. In addition, superficial adsorption does not need additional modifications such as coating with inorganic and organic biomaterials, which will eliminate additional exogenic materials and costs to achieve the approval of FDA for clinical application. However, most of the clinically available CaP-based materials, such as TCP and BCP, do not bear a favorable physicochemical surface property that enables a slow release profile of BMP2. Therefore, most of the thereon superficially adsorbed BMP2 are released and exhausted too rapidly and fail to efficiently induce new bone formation [33–35]. Furthermore, the transiently high concentration of BMP2 may cause a series of unintended adverse effects [19]. Due to these limitations, continuous efforts have been undertaken to develop novel synthetic materials with advanced physicochemical and biological properties [36, 37]. In this study, we adopted NHA blocks that are clinically available and bear a significantly enhanced surface to potentially facilitate the slow release of superficially adsorbed BMP2. In our study, we, for the first time, proved that the NHA blocks could enable a slow release of superficially adsorbed BMP2 and promote new bone formation. Our results indicated a possibility of NHA blocks combined with BMP2 to treat large-volume bone defects.

The surface of hydroxyapatite has a high adsorption ability for many substances. It is a common absorbent in chromatography used to separate and purify proteins. In particular, NHA shows a significantly higher capacity for adsorbing proteinous agents in comparison with microphased hydroxyapatite [38]. It had been reported that 2 mg of NHA adsorbs more than 99.9% of 1 $\mu$g/ml BMP2 in 0.5 ml PBS within 24 h [39]. This suggests that NHA is a potential carrier for proteins. Due to its similar loading and release kinetics to BMP2, BSA is often employed as a model protein to mimic a BMP2 loading and release assay [40]. In this study, the loading efficiency of a proteinous agent (FITC-BSA) was positively correlated with the concentrations of BMP2 (Figure 1(b)). The success of incorporation was confirmed with fluorescence images of cross sections indicating that the protein distributed 1 mm beneath the surface (Figure 1(a)). BSA was sustainably released up to day 35 from different concentrations of BSA-loaded NHA. In our previous studies, the FITC-BSA that was superficially adsorbed onto another clinically widely used CaP-based material (deproteinized bovine bone) was exhausted within 13 days [16]. Our finding demonstrated the superior ability

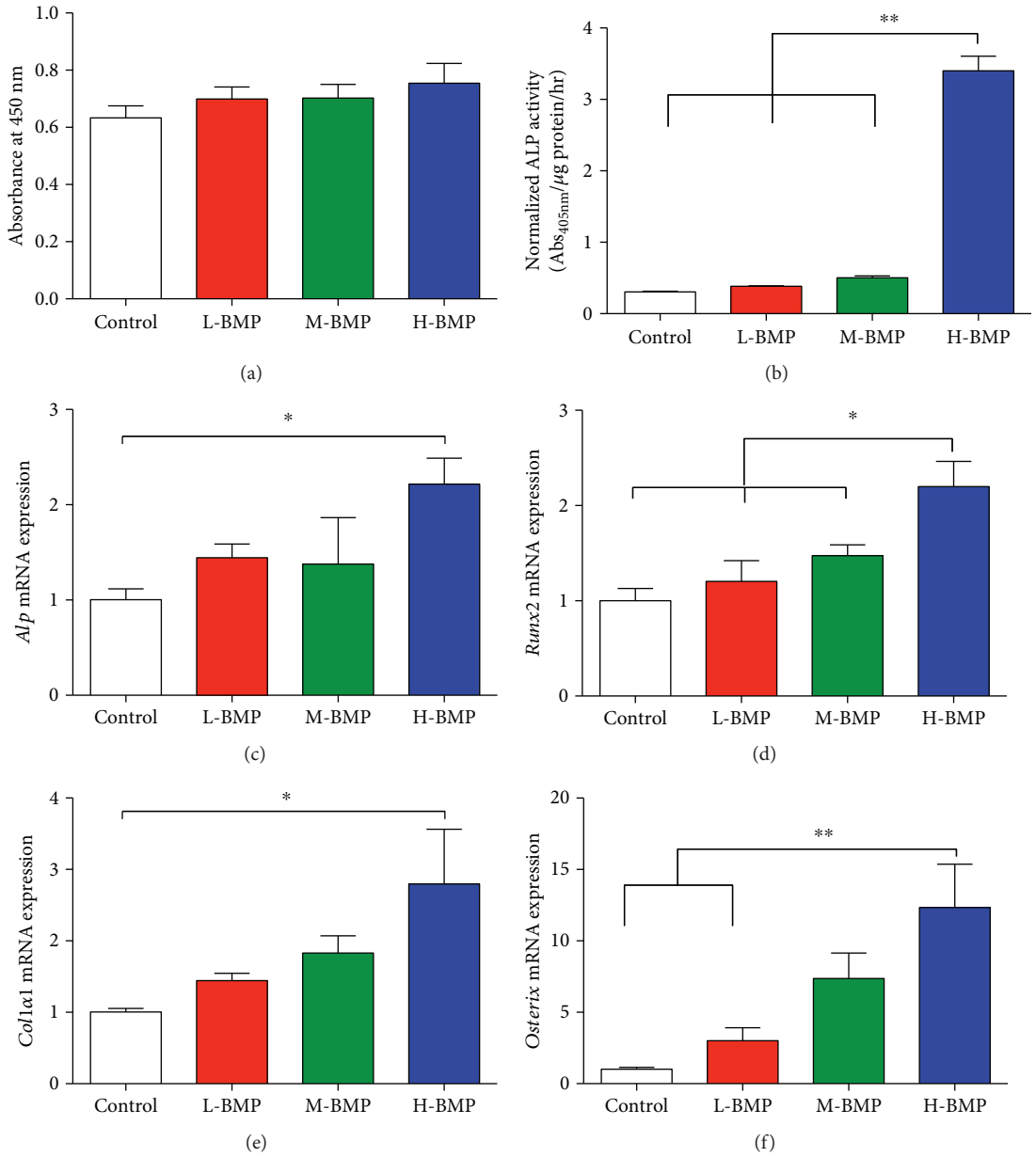


Figure 2: NHA incorporated with rhBMP2 enhanced osteogenic differentiation of C2C12 cells in vitro. (a) Cell proliferation and (b) ALP activity. Gene expression of (c) *Alp*, (d) *Runx2*, (e) *Col1α1*, and (f) *Osterix* in C2C12 cells at day 7. Data are presented as the mean ± SD, $n = 8$. Significant effect of the treatment, $^{*}p < 0.05$ and $^{**}p < 0.01$. *Alp*: alkaline phosphatase, *Runx2*: Runt-Related Transcription Factor 2, *Col1α1*: collagen 1 alpha 1.

of NHA to give sustained release of growth protein compared to that of deproteinized bovine bone containing natural hydroxyapatite [41].

In this study, the bioactivities of the released BMP2 from NHA blocks were assayed using C2C12 cells. The BMP2 loading did not affect the cell viability (Figure 2(a)). In contrast, the osteogenic early differentiation marker—ALP activity—was significantly enhanced in the high-dose BMP2-loaded NHA group (Figure 2(b)). Consistently, the mRNA expression of *Alp*, *Col1α1*, *Runx2*, and *Osterix* was also significantly enhanced in the high-dose BMP2-loaded NHA group compared to the control group (Figures 2(c)–2(f)). The result indicated that the BMP2 adsorbed onto NHA retained its bioactivity. However, low- and medium-dose BMP2-loaded NHA did not affect the osteogenic differentiation of C2C12 cells. This might be due to the cell type used and culture conditions, i.e., C2C12 cells are of myoblast origin and are cultured without an osteogenic medium. We adapted this cell model and method for an in vitro study to mimic our in vivo ectopic model. The osteoinductive potential of low- and medium-dose BMP2-loaded NHA osteogenic in precursor cells cultured with osteogenic medium might be more pronounced compared to the present culture model.

The golden standard of biomaterial osteoinductivity is considered to be the ability to form bone tissue in ectopic sites [42]. Therefore, we analyzed the osteoinductive effect

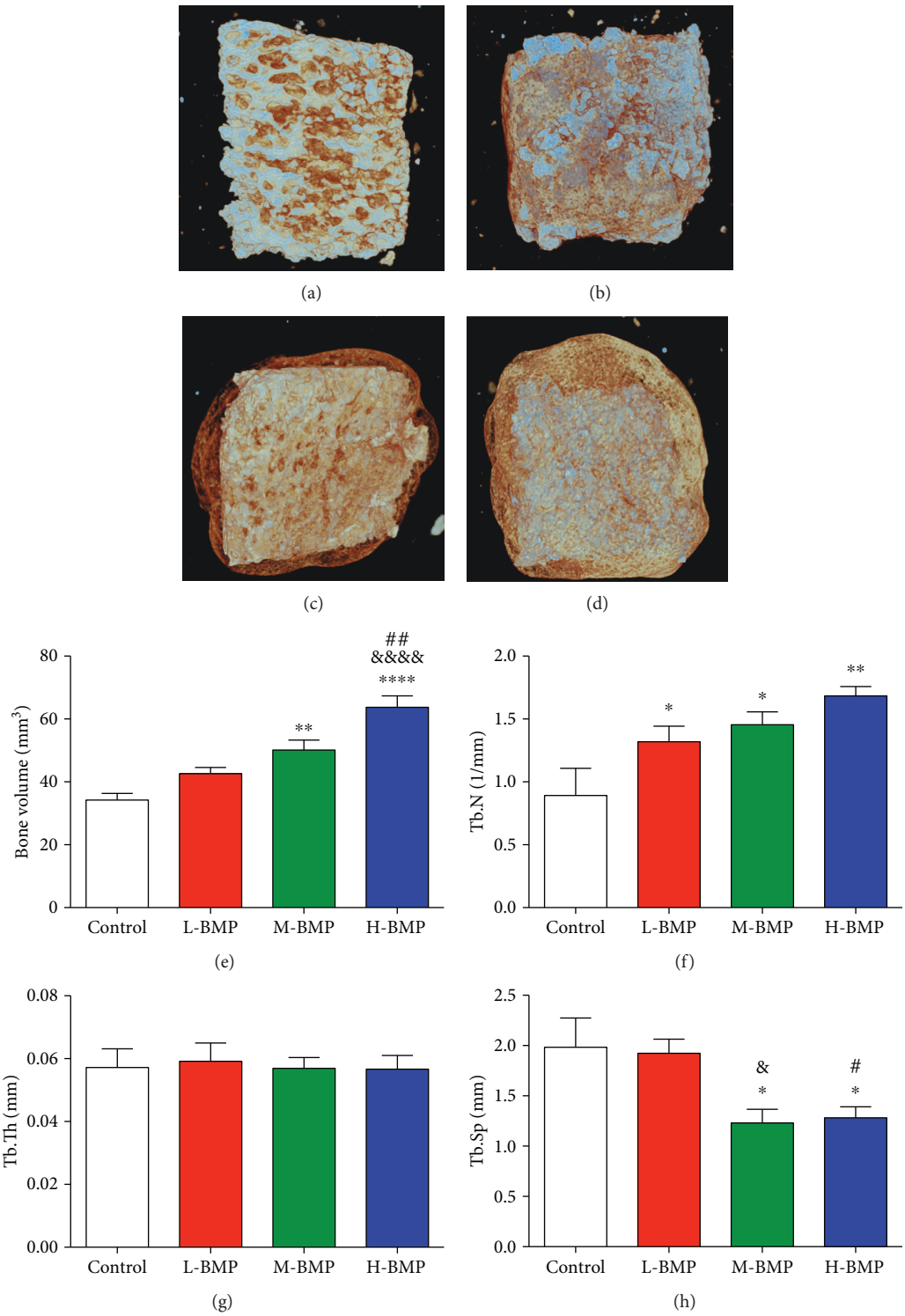


Figure 3: Representative $\mu$-CT images of (a) NHA, (b) L-BMP2-NHA, (c) M-BMP2-NHA, and (d) H-BMP2-NHA implanted subcutaneously in mice at week 4. Quantitative analysis of newly formed bone and trabecular parameters: (e) bone volume, (f) Tb.N, (g) Tb.Th, and (h) Tb.Sp. Data are presented as the mean ± SD, $n = 8$. Significant effect of the treatment: compared to control, $^{*}p < 0.05$ and $^{**}p < 0.01$, compared to L-BMP, $^{\&}p < 0.05$ and $^{\&\&\&\&}p < 0.0001$, and compared to M-BMP, $^{\#\#}p < 0.01$. L: low dose, M: medium dose, H: high dose.

of BMP2-loaded NHA on bone formation in mice subcutaneous graft. The volume density of newly formed bone was positively correlated with the concentration of BMP2. New bone formation was not observed in the control group, which might be due to a lack of osteoinduction. An ectopic site lacks growth factors and precursor cells from a bony environment.

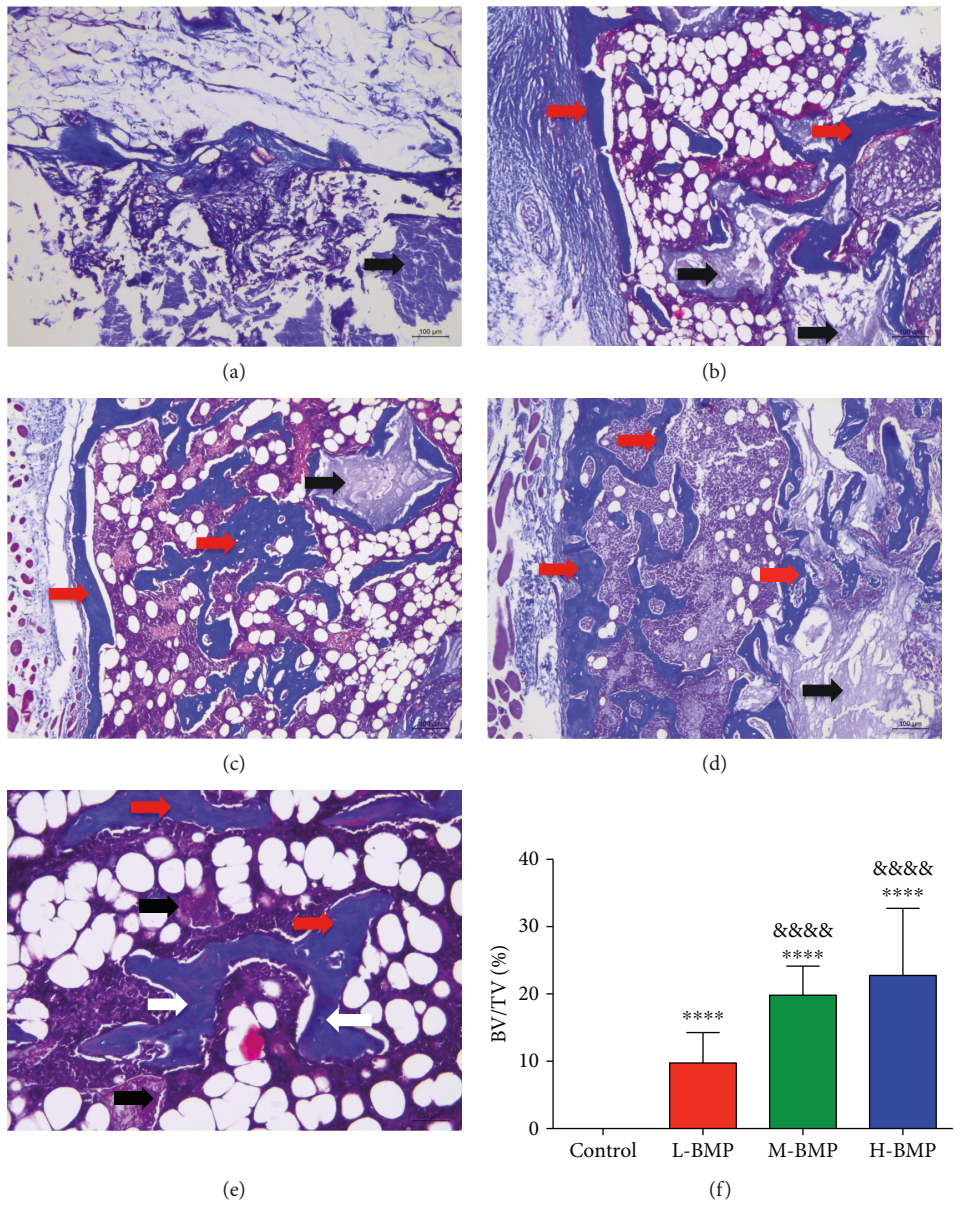


Figure 4: Representative images of histological tissue sections: (a) NHA, (b) L-BMP2-NHA, (c) M-BMP2-NHA, and (d) H-BMP2-NHA implants. (e) Higher magnification of image in (d). (f) Quantitative analysis of the BV/TV ratio. Scale bars in (a), (b), (c), and (d): 100 $\mu$m. Scale bar in (e): 50 $\mu$m. The sections were stained with Masson's trichrome staining. The red arrows indicate the blue collagen fibers in the newly formed bone. The white arrows indicate the lacunae. The black arrows indicate the residual material. Data are presented as the mean ± SD, $n = 8$. Significant effect of the treatment compared to control, $^{****}p < 0.0001$, and compared to L-BMP, $^{\&\&\&\&}p < 0.0001$. BV/TV: bone volume over total volume ratio.

Therefore, BMP2 incorporation is essential for osteogenesis in an ectopically implanted bone graft. Medium and high doses of BMP2-loaded NHA robustly enhanced bone regeneration compared to the control and low-dose BMP2-loaded NHA groups. A similar effect was observed on newly formed bone trabecular parameters. Since the BMP2-loaded NHA was able to enhance bone formation even at the ectopic site, the osteoinductive effect of BMP2-loaded NHA might be more pronounced in bone defects.

The animal-originated collagen sponge proves to be a good carrier for BMP in clinical practice to treat small-sized defects. After being soaked in BMP2 solution for 15 minutes, the collagen sponge had been reported to load with approximately 95% of the rhBMP2 and release the protein over about a 2-week period, with a half-life of 2–3 days [43]. Since a high dose of BMP2 is required, the collagen sponge could not be a cost-effective BMP2 delivery system for large-volume bone defects. Moreover, in repairing large-volume bone defects, the collagen sponge alone is not able to provide enough mechanical stability. More rigid materials have to be applied as supporting scaffolds along with the protein and its carrier. In this study, we showed that NHA blocks could carry BMP2 at a very high loading efficiency, retain its activity, and efficaciously induce new bone formation even in a subcutaneous

profibrotic environment. These findings indicated a very promising application potential for the BMP2-NHA bone graft to treat large-volume bone defects in clinical settings. A limitation of this study is the use of FITC-BSA instead of BMP2 for the in vitro drug loading and release assay. Although many previous studies had adapted this method, FITC-BSA might not have exactly the same loading and release properties as BMP2. In spite of the high cost, many researchers prefer the direct use of BMP2 to analyze the loading and release assay more accurately. Another limitation of this study is the lack of an in vivo bone defect healing experiment. Since the implantation of a BMP2-NHA graft in the bone defect provides interactions between BMP2, biomaterial, and host bone tissue, we recommend a future study focusing on these issues.

## 5. Conclusions

In the present study, NHA showed the capacity to retain the adsorbed protein efficiently and release them in a sustained fashion in vitro. BMP2-loaded NHA was biocompatible and induced osteogenic differentiation of C2C12 cells in vitro. Different doses of BMP2-loaded NHA enhanced bone regeneration in the mice ectopic model in a dose-dependent manner. Our in vitro and in vivo findings suggest that NHA is an efficient carrier of osteoinductive growth factors. The biocompatible, osteoconductive, and osteoinductive properties of BMP2-loaded NHA suggest that it is a potent bone graft for treating large-volume bone defects.

## Data Availability

The data used to support the findings of this study are included within the article.

## Conflicts of Interest

The authors declare that they have no conflicts of interest.

## Authors' Contributions

Miao Zhou and Yuan-ming Geng contributed equally to this work.

## Acknowledgments

The authors thank Shuai shuai Cao and Hui Zhou for the release assay experiment and Professor Hendrick Terheyden for his guidance during study design. The study was financially supported by the National Key Research and Development Program of China (No. 2016YFC1102900), Guangzhou Science, Technology, and Innovation Commission (No. 201704030024), the Science Foundation for the Youth Scholars of Southern Medical University (No. PY2015N018) and the International Team for Implantology (No. 8812012).

## References

[1] E. Garcia-Gareta, M. J. Coathup, and G. W. Blunn, "Osteoinduction of bone grafting materials for bone repair and regeneration," *Bone*, vol. 81, pp. 112–121, 2015.

[2] A. M. Jakoi, J. A. Iorio, and P. J. Cahill, "Autologous bone graft harvesting: a review of grafts and surgical techniques," *Musculoskeletal Surgery*, vol. 99, no. 3, pp. 171–178, 2015.

[3] C. Delloye, O. Cornu, V. Druez, and O. Barbier, "Bone allografts: what they can offer and what they cannot," *The Journal of Bone and Joint Surgery British Volume*, vol. 89-B, no. 5, pp. 574–580, 2007.

[4] S. M. Graham, A. Leonidou, N. Aslam-Pervez et al., "Biological therapy of bone defects: the immunology of bone allo-transplantation," *Expert Opinion on Biological Therapy*, vol. 10, no. 6, pp. 885–901, 2010.

[5] Y. C. Chai, A. Carlier, J. Bolander et al., "Current views on calcium phosphate osteogenicity and the translation into effective bone regeneration strategies," *Acta Biomaterialia*, vol. 8, no. 11, pp. 3876–3887, 2012.

[6] F. Gouin, F. Yaouanc, D. Waast, B. Melchior, J. Delecrin, and N. Passuti, "Open wedge high tibial osteotomies: calcium-phosphate ceramic spacer versus autologous bone-graft," *Orthopaedics & Traumatology: Surgery & Research*, vol. 96, no. 6, pp. 637–645, 2010.

[7] T. Angelo, W. Marcel, K. Andreas, and S. Izabela, "Biomechanical stability of dental implants in augmented maxillary sites: results of a randomized clinical study with four different biomaterials and PRF and a biological view on guided bone regeneration," *BioMed Research International*, vol. 2015, Article ID 850340, 17 pages, 2015.

[8] A. de Ruiter, N. Janssen, R. van Es et al., "Micro-structured beta-tricalcium phosphate for repair of the alveolar cleft in cleft lip and palate patients: a pilot study," *The Cleft Palate-Craniofacial Journal*, vol. 52, no. 3, pp. 336–340, 2015.

[9] L. Ohayon, S. Taschieri, S. Corbella, and M. del Fabbro, "Maxillary sinus floor augmentation using biphasic calcium phosphate and a hydrogel polyethylene glycol covering membrane: an histological and histomorphometric evaluation," *Implant Dentistry*, vol. 25, no. 5, pp. 599–605, 2016.

[10] M. Andratschke and H. Hagedorn, "First results of frontal sinus obliteration with a synthetic, resorbable and osteoconductive bone graft of $\beta$-tricalcium phosphate," *The Journal of Laryngology & Otology*, vol. 131, no. 6, pp. 534–540, 2017.

[11] T. Okada, T. Kanai, N. Tachikawa, M. Munakata, and S. Kasugai, "Histological and histomorphometrical determination of the biogradation of $\beta$-tricalcium phosphate granules in maxillary sinus floor augmentation: a prospective observational study," *Implant Dentistry*, vol. 26, no. 2, pp. 275–283, 2017.

[12] A. Abarrategi, C. Moreno-Vicente, V. Ramos, I. Aranaz, J. V. Sanz Casado, and J. L. López-Lacomba, "Improvement of porous $\beta$-TCP scaffolds with rhBMP-2 chitosan carrier film for bone tissue application," *Tissue Engineering Part A*, vol. 14, no. 8, pp. 1305–1319, 2008.

[13] R. M. Gruber, S. Krohn, C. Mauth et al., "Mandibular reconstruction using a calcium phosphate/polyethylene glycol hydrogel carrier with BMP-2," *Journal of Clinical Periodontology*, vol. 41, no. 8, pp. 820–826, 2014.

[14] P. Y. Yun, Y. K. Kim, K. I. Jeong, J. C. Park, and Y. J. Choi, "Influence of bone morphogenetic protein and proportion of hydroxyapatite on new bone formation in biphasic calcium

phosphate graft: two pilot studies in animal bony defect model," *Journal of Cranio-Maxillofacial Surgery*, vol. 42, no. 8, pp. 1909–1917, 2014.

[15] Y. Liu, R. O. Huse, K. de Groot, D. Buser, and E. B. Hunziker, "Delivery mode and efficacy of BMP-2 in association with implants," *Journal of Dental Research*, vol. 86, no. 1, pp. 84–89, 2007.

[16] G. Wu, E. B. Hunziker, Y. Zheng, D. Wismeijer, and Y. Liu, "Functionalization of deproteinized bovine bone with a coating-incorporated depot of BMP-2 renders the material efficiently osteoinductive and suppresses foreign-body reactivity," *Bone*, vol. 49, no. 6, pp. 1323–1330, 2011.

[17] J. Tazaki, M. Murata, T. Akazawa et al., "BMP-2 release and dose-response studies in hydroxyapatite and $\beta$-tricalcium phosphate," *Bio-Medical Materials and Engineering*, vol. 19, no. 2-3, pp. 141–146, 2009.

[18] P. Hänseler, M. Ehrbar, A. Kruse et al., "Delivery of BMP-2 by two clinically available apatite materials: in vitro and in vivo comparison," *Journal of Biomedical Materials Research Part A*, vol. 103, no. 2, pp. 628–638, 2015.

[19] Z. S. Haidar, R. C. Hamdy, and M. Tabrizian, "Delivery of recombinant bone morphogenetic proteins for bone regeneration and repair. Part A: current challenges in BMP delivery," *Biotechnology Letters*, vol. 31, no. 12, pp. 1817–1824, 2009.

[20] B. Poon, T. Kha, S. Tran, and C. R. Dass, "Bone morphogenetic protein-2 and bone therapy: successes and pitfalls," *Journal of Pharmacy and Pharmacology*, vol. 68, no. 2, pp. 139–147, 2016.

[21] S. Dietze, T. Bayerlein, P. Proff, A. Hoffmann, and T. Gedrange, "The ultrastructure and processing properties of Straumann Bone Ceramic and NanoBone," *Folia Morphologica*, vol. 65, no. 1, pp. 63–65, 2006.

[22] Q. Liu, T. Douglas, C. Zamponi et al., "Comparison of in vitro biocompatibility of NanoBone® and BioOss® for human osteoblasts," *Clinical Oral Implants Research*, vol. 22, no. 11, pp. 1259–1264, 2011.

[23] M. Wiens, T. A. Elkhooly, H.-C. Schröder, T. H. A. Mohamed, and W. E. G. Müller, "Characterization and osteogenic activity of a silicatein/biosilica-coated chitosan-graft-polycaprolactone," *Acta Biomaterialia*, vol. 10, no. 10, pp. 4456–4464, 2014.

[24] G. Fielding and S. Bose, "$SiO_2$ and ZnO dopants in three-dimensionally printed tricalcium phosphate bone tissue engineering scaffolds enhance osteogenesis and angiogenesis in vivo," *Acta Biomaterialia*, vol. 9, no. 11, pp. 9137–9148, 2013.

[25] D. Inzunza, C. Covarrubias, A. V. Marttens et al., "Synthesis of nanostructured porous silica coatings on titanium and their cell adhesive and osteogenic differentiation properties," *Journal of Biomedical Materials Research Part A*, vol. 102, no. 1, pp. 37–48, 2014.

[26] G. A. Gholami, B. Najafi, F. Mashhadiabbas, W. Goetz, and S. Najafi, "Clinical, histologic and histomorphometric evaluation of socket preservation using a synthetic nanocrystalline hydroxyapatite in comparison with a bovine xenograft: a randomized clinical trial," *Clinical Oral Implants Research*, vol. 23, no. 10, pp. 1198–1204, 2012.

[27] M. Wolf, A. Wurm, F. Heinemann et al., "The effect of patient age on bone formation using a fully synthetic nanocrystalline bone augmentation material in maxillary sinus grafting," *The International Journal of Oral & Maxillofacial Implants*, vol. 29, no. 4, pp. 976–983, 2014.

[28] J. Lorenz, K. Eichler, M. Barbeck et al., "Volumetric analysis of bone substitute material performance within the human sinus cavity of former head and neck cancer patients: a prospective, randomized clinical trial," *Annals of Maxillofacial Surgery*, vol. 6, no. 2, pp. 175–181, 2016.

[29] K. Abshagen, I. Schrodi, T. Gerber, and B. Vollmar, "In vivo analysis of biocompatibility and vascularization of the synthetic bone grafting substitute NanoBone," *Journal of Biomedical Materials Research Part A*, vol. 91A, no. 2, pp. 557–566, 2009.

[30] C. Harms, K. Helms, T. Taschner et al., "Osteogenic capacity of nanocrystalline bone cement in a weight-bearing defect at the ovine tibial metaphysis," *International Journal of Nanomedicine*, vol. 7, pp. 2883–2889, 2012.

[31] E. Rumpel, E. Wolf, E. Kauschke et al., "The biodegradation of hydroxyapatite bone graft substitutes in vivo," *Folia Morphologica*, vol. 65, no. 1, pp. 43–48, 2006.

[32] F. G. Draenert, A.-L. Nonnenmacher, P. W. Kämmerer, J. Goldschmitt, and W. Wagner, "BMP-2 and bFGF release and in vitro effect on human osteoblasts after adsorption to bone grafts and biomaterials," *Clinical Oral Implants Research*, vol. 24, no. 7, pp. 750–757, 2013.

[33] A. Abarrategi, C. Moreno-Vicente, F. J. Martínez-Vázquez et al., "Biological properties of solid free form designed ceramic scaffolds with BMP-2: in vitro and in vivo evaluation," *PLoS One*, vol. 7, no. 3, article e34117, 2012.

[34] H. Autefage, F. Briand-Mésange, S. Cazalbou et al., "Adsorption and release of BMP-2 on nanocrystalline apatite-coated and uncoated hydroxyapatite/$\beta$-tricalcium phosphate porous ceramics," *Journal of Biomedical Materials Research Part B: Applied Biomaterials*, vol. 91B, no. 2, pp. 706–715, 2009.

[35] S. Kissling, M. Seidenstuecker, I. H. Pilz, N. P. Suedkamp, H. O. Mayr, and A. Bernstein, "Sustained release of rhBMP-2 from microporous tricalciumphosphate using hydrogels as a carrier," *BMC Biotechnology*, vol. 16, no. 1, p. 44, 2016.

[36] K. Lin, L. Xia, J. Gan et al., "Tailoring the nanostructured surfaces of hydroxyapatite bioceramics to promote protein adsorption, osteoblast growth, and osteogenic differentiation," *ACS Applied Materials & Interfaces*, vol. 5, no. 16, pp. 8008–8017, 2013.

[37] J. Venkatesan and S. K. Kim, "Nano-hydroxyapatite composite biomaterials for bone tissue engineering—a review," *Journal of Biomedical Nanotechnology*, vol. 10, no. 10, pp. 3124–3140, 2014.

[38] N. Ribeiro, S. R. Sousa, and F. J. Monteiro, "Influence of crystallite size of nanophased hydroxyapatite on fibronectin and osteonectin adsorption and on MC3T3-E1 osteoblast adhesion and morphology," *Journal of Colloid and Interface Science*, vol. 351, no. 2, pp. 398–406, 2010.

[39] C. S. Goonasekera, K. S. Jack, G. Bhakta et al., "Mode of heparin attachment to nanocrystalline hydroxyapatite affects its interaction with bone morphogenetic protein-2," *Biointerphases*, vol. 10, no. 4, 2015.

[40] P. Yilgor, N. Hasirci, and V. Hasirci, "Sequential BMP-2/BMP-7 delivery from polyester nanocapsules," *Journal of Biomedical Materials Research Part A*, vol. 93, no. 2, pp. 528–536, 2010.

[41] J. Tuukkanen and M. Nakamura, "Hydroxyapatite as a nanomaterial for advanced tissue engineering and drug therapy," *Current Pharmaceutical Design*, vol. 23, no. 26, pp. 3786–3793, 2017.

[42] R. J. Miron and Y. F. Zhang, "Osteoinduction: a review of old concepts with new standards," *Journal of Dental Research*, vol. 91, no. 8, pp. 736–744, 2012.

[43] B. McKay, "Local sustained delivery of recombinant human bone morphogenetic protein-2 (rhBMP-2)," in *2009 Annual International Conference of the IEEE Engineering in Medicine and Biology Society*, pp. 236-237, Minneapolis, MN, USA, 2009.